AFM reveals the interaction and nanoscale effects imposed by squalamine on Staphylococcus epidermidis

Sofiane El-Kirat-Chatel, Mihayl Varbanov, Chloé Retourney, Elsa Salles, Arnaud Risler, Jean-Michel Brunel, Audrey Beaussart

Submitted to Colloids and Surfaces B

AFM reveals the interaction and nanoscale effects imposed by squalamine on *Staphylococcus epidermidis*

Sofiane EL-Kirat-Chatel[1]*, Mihayl Varbanov[2,3], Chloé Retourney[1], Elsa Salles[4], Arnaud Risler[2], Jean-Michel Brunel[5], Audrey Beaussart[6]*

[1]Université de Lorraine, CNRS, LCPME, F-54000 Nancy, France
[2]Université de Lorraine, CNRS, L2CM, F-54000 Nancy, France
[3] Laboratoire de Virologie, CHRU de Nancy Brabois, F-54500 Vandœuvre-lès-Nancy, France
[4]Université de Lorraine, CNRS, LIEC, F-57000 Metz, France
[5]UMR_MD1, U-1261, Aix Marseille Université, INSERM, SSA, MCT, Marseille, France
[6]Université de Lorraine, CNRS, LIEC, F-54000 Nancy, France

* Corresponding author:
elkirat1@univ-lorraine.fr
audrey.beaussart@univ-lorraine.fr

ORCID
A. Beaussart: 0000-0002-4602-3019
S. El-Kirat-Chatel: 0000-0001-5877-5640

Table of Contents Graphic

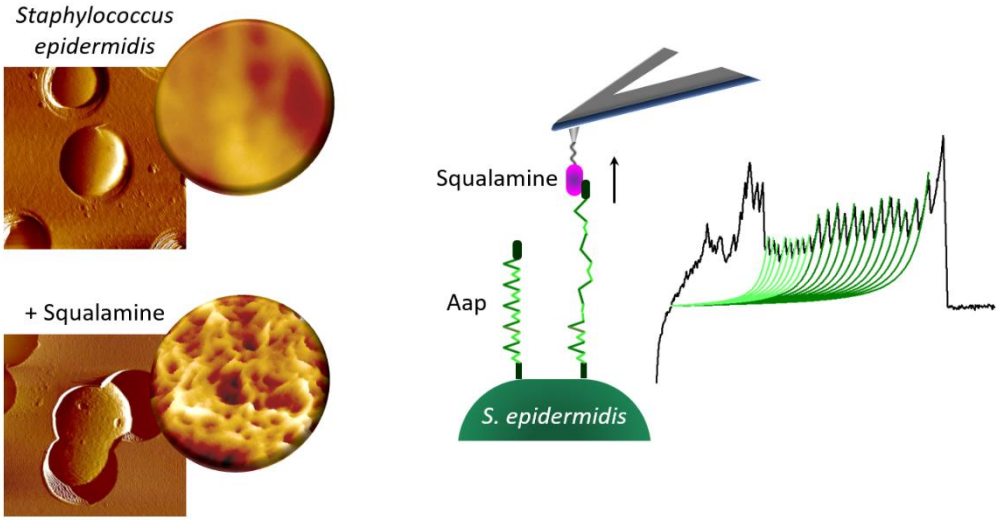

ABSTRACT

The Gram-positive bacterium *Staphylococcus epidermidis* is responsible for important nosocomial infections. With the continuous emergence of antibiotic-resistant strains, the search for new treatments has been amplified in the last decades. A potential candidate against multidrug-resistant bacteria is squalamine, a natural amino-sterol discovered in dogfish sharks. Despite its broad-spectrum efficiency, little is known about squalamine mode of action. Here, we used atomic force microscopy (AFM) imaging to decipher the effect of squalamine on *S. epidermidis* morphology, revealing the peptidoglycan structure at the bacterial surface after the drug action. Single-molecule force spectroscopy with squalamine-decorated tips shows that squalamine binds to the cell surface *via* the spermidine motif, most likely through electrostatic interactions between the amine groups of the molecule and the negatively-charged bacterial cell wall. We demonstrated that - although spermidine is sufficient for the initial attachment of squalamine to *S. epidermidis* – the integrity of the molecule needs to be conserved for its antimicrobial action. Deeper analysis of the AFM force-distance signatures revealed the implication of the accumulation-associated protein (Aap), one of the main adhesins of *S. epidermidis*, in the initial binding of squalamine to the bacterial cell wall. This works highlights that AFM -combined with microbiological assays at the bacterial suspension scale- is a valuable approach to better understand the molecular mechanisms behind the efficiency of squalamine antibacterial activity.

Keywords: *Staphylococcus epidermidis*, squalamine, atomic force microscopy, interactions, antimicrobial, aminosterol, Aap

Introduction

The human skin commensal *Staphylococcus epidermidis* has developed as one of the leading opportunistic pathogens responsible for nosocomial infections. The bacteria gain access to the body mostly by adhering and proliferating on indwelling medical devices [1,2]. The initial adhesion on such abiotic surfaces are mediated by a small collection of surface-associated proteins named adhesins, including the accumulation associated protein Aap [3-6]. Aap is composed of N-terminal repeats followed by a lectin like domain (collectively called the A domain), and a B domain containing 5 to 17 conserved repeats, each of them being made of a 72-amino acids (aa) G5 segment and a 48-aa E segment. The A region has been identified as responsible for the initial binding to host surfaces, whereas the B domain controls intercellular adhesion [3,7].

Although *S. epidermidis* contaminations are generally not life-threatening, their frequency and difficulty to be eradicated constitute a major health concern. In addition to their strong ability to colonize medical devices, the complication arises mostly from the existence of specific antibiotic resistance genes that render *S. epidermidis* insensitive to classical treatments such as methicillin, rifamycin, gentamicin or chloramphenicol [8]. In the search of new classes of potential antimicrobials limiting the progress of drug-resistant microbes, membrane-targeting antibiotics have been suggested as promising candidates. Among them, squalamine, a natural aminosterol isolated from dogfish shark has appeared as remarkably attractive due to its broad-spectrum activity and efficiency against multidrug resistant bacteria [9-12]. This membrane-active molecule would disrupt the outer membranes of Gram-negative bacteria in a detergent-like mechanism of action, and would depolarize the bacterial membranes of Gram-positive bacteria [11-13]. Squalamine is composed of a sterol

core with a sulfated side chain, a hydrophilic polyamine spermidine moiety bonded to a hydrophobic unit. Due to the low abundance of natural squalamine, many synthetic amino-steroid derivatives have been synthesized and tested, revealing *e.g.*, that the sulfate group has a low influence on their antimicrobial activity [11-13]. The positively-charged amino groups of the drug is likely to bind to the negatively charged lipopolysaccharides (LPS) at the cellular surface of Gram-negative bacteria. However, the initial attachment of squalamine to Gram-positive bacteria, devoid of LPS, remains less understood [9,13].

Here, we used a combination of biological assays, fluorescence test and different AFM modalities to decipher the mechanisms of squalamine adhesion to the surface of *S. epidermidis* and the subsequent consequence on the cell morphology. Squalamine treatment close to inhibitory concentrations causes increase of cell roughness and appearing of the peptidoglycan structure at the surface of the treated bacteria. Using AFM-based force spectroscopy measurements, we showed that the presence of the positively-charged spermidine group is necessary for the initial attachment of squalamine to the biosurface, but that the motif itself is not sufficient for the antimicrobial action of the molecule. We also demonstrated that the adhesin Aap is involved in the primarily attachment of the drug to the bacterial cell wall.

MATERIALS AND METHODS

Microorganisms and Culture Media

The American Type Culture Collection (ATCC) *S. epidermidis* strain (ATCC-14990) was purchased from LGC Standards, Molsheim, France and used for the *in vitro* antibacterial evaluation and AFM experiments. Mueller-Hinton Cation-Adjusted Agar (MHA-CA, Becton Dickinson) and Broth (MHB-CA, Becton Dickinson) were used for bacterial growth and antimicrobial assays. Bacteria were grown at 35°C for 18 hours.

Squalamine was kindly provided by Dr. JM Brunel (Aix Marseille Université, INSERM, SSA, MCT, Marseille, France). Stock solutions were prepared in sterile water. The stock solution was subsequently diluted for use as a working solution.

Antibacterial Assay

The minimum inhibitory concentrations (MIC) values of the molecules were determined using the microdilution technique according to the NF EN ISO 20776-1 guidelines (ISO 20776-1:2019). Susceptibility testing of infectious agents and evaluation of performance of antimicrobial susceptibility test devices — Part 1: Broth micro-dilution reference method for testing the in vitro activity of antimicrobial agents against rapidly growing aerobic bacteria involved in infectious diseases). In brief, 50 µL of water-diluted Squalamine at 128 µM were added to an equal volume of MHB-CA. Initially, 50 µL of this solution were serially diluted in 50 µL MHB-CA. Then, 50 µL of bacteria at 10^6 colony forming units per mL (CFU/mL) were added. Final molecule concentration was ranging from 0.1 to 32 µM. The final inoculum was 5.10^5 CFU/mL and was checked according to ISO guidelines. MIC was determined as the lowest concentration with no visible bacterial growth after an 18 h incubation at 35°C. Each test consists in 8 repetitions. When MIC was obtained, a minimal bactericidal concentration

(MBC) test was performed. Cells were plated with product at MIC, double MIC, four MIC; and incubated overnight at 35°C on Mueller Hinton Agar (BD, 225250, New York, US). The same approach was used in the determination of MIC and MBC of spermidine.

Cytotoxicity evaluation

The cytotoxicity of squalamine was determined using the MTT (3-(4,5-dimethylthiazol-2-yl)-2,5-diphenyltetrazolium bromide) colorimetric assay, as previously described [14]. The effect of the molecule on the viability of normal human lung fibroblasts MRC-5 (MRC-5, ATCC® CCL-171TM, Public Health England, Salisbury, England) cells was thus determined. The cells were cultured in Minimal Essential Medium (MEM, M4655, Sigma-Aldrich, France) supplemented with 2% fetal calf serum (CVFSV F00-0U, Eurobio, France). The treated cells were incubated at 37°C in 5% CO_2 atmosphere for 72 h. The absorbance of the solution was measured at 540 nm. The absorbance values were proportional to the surviving cells and the cytotoxic concentration (CC) for Squalamine was calculated to be 10 µM, allowing the survival of more than 50% of the host cells. The MIC values of Squalamine against *S. epidermidis* and the CC values of the compound against the MRC-5 cells were used to determine the selectivity index (SI) for the molecule using the following formula: SI = CC / MIC.

Atomic force microscopy measurements.

AFM measurements were performed at room temperature in Tris buffer (Tris 100mM 150mM NaCl pH=7.4) using a Fastscan dimension Icon with Nanoscope V controller (Bruker) and a Bioscope Resolve AFM (Bruker corporation, Santa Barbara, CA). Bacteria from the cell suspension prepared as detailed above were centrifuged (2 min, 2000 rpm) and resuspended in Tris buffer twice, and then filtered through a polycarbonate porous membrane (Millipore,

147 Billerica, MA, pore size: 1.2 µm) with pore size similar to the cell diameter. The filter was
148 gently rinsed with the buffer, carefully cut (~ 1 cm x 1 cm), attached to a steel sample puck
149 using a small piece of double-sided adhesive tape and mounted into the AFM liquid cell
150 without de-wetting. Images were acquired in Peak Force Tapping mode using NPG silicon
151 nitride tips (Bruker), with a peak force frequency of 2 kHz, a peak force amplitude of 150 nm,
152 a scan rate of 2 Hz and a setpoint of 1 nN. RMS (root mean square) values were determined
153 using Nanoscope analysis software (Bruker; Rq values on 300 nm x 300 nm images after
154 second order flattening). For squalamine-treated cells, bacteria were grown overnight in
155 Muller-Hinton broth as described above, rinsed twice in Tris buffer, and resuspended in
156 Muller-Hinton broth at OD= 1. Squalamine was then added at the desired concentration (*i.e.*
157 1 µM for 0.5XMIC; 2 µM for MIC; 4 µM for 2XMIC) and cells were then cultivated for 12 hours in
158 the conditions described above.

159 Prior to each force spectroscopy measurement, a calibration was performed on a rigid
160 substratum in order to determine the deflection sensitivity (nm/V) of the AFM tip. In turn,
161 this leads to the accurate evaluation of the cantilever spring constant following thermal
162 noise method. For single-molecule force spectroscopy experiments, AFM tips were
163 functionalized with squalamine or spermidine by covalent grafting using N-
164 hydroxysuccinimide (NHS)/ 1-ethyl-3-(3-dimethylaminopropyl)-carbodiimide (EDC)
165 chemistry. For that purpose, gold-coated AFM tips (NPG, Bruker) were cleaned in UV-ozone
166 incubator for 10 minutes, rinsed with ethanol, and immersed overnight in a 1 mM 16-
167 mercaptohexadecanoic acid thiols (Sigma) diluted in ethanol, rinsed with ethanol and dry
168 with nitrogen. They were then immersed in 4 mL of ultrapure water containing 40 mg of NHS
169 (Sigma) and 100 mg of EDC (Sigma). After 30 min, tips were rinsed in ultrapure water and
170 immersed in the squalamine or spermidine suspension at 0.2 mg/mL for 1 hour, rinsed and

stored in Tris buffer until use. Hydrophobic tips were obtained by immersing clean gold-coated tips overnight in a 1 mM 1-dodecanehiol (Sigma) diluted in ethanol, rinsed with ethanol and dry with nitrogen.

All force spectroscopy experiments were performed in Tris buffer. Adhesion maps were obtained by recording 32 x 32 force -distance curves on 500 nm x 500 nm area at the bacterial surface, with a maximum applied force of 250 pN and a constant approach and retraction tip speed of 1 µm s^{-1}. Adhesion maps were reconstructed by calculating the adhesion force of the last peak of each force curve and displaying the value as a colour/grey pixel.

Results and discussion

Squalamine has antimicrobial and bactericidal effects

We first determined the minimum inhibitory concentration (MIC) of squalamine on *S. epidermidis*. For that purpose, we tested the antimicrobial activity of 9 different concentrations of squalamine, ranging from 32 to 0.1 µM, and determined the MIC as the minimum concentration of squalamine were no bacterial growth was observed. As shown on Fig. 1B and Fig. 1 SI, the MIC was obtained for a squalamine concentration of 2 µM.

The cytotoxic concentration (CC) for squalamine allowing the survival of more than 50 % of the MRC-5 cells was 10 µM. The results show that squalamine has a selectivity index (SI) value (SI = CC/MIC) of 5 for *S. epidermidis* (Fig. 1 SI). A selectivity index value greater than 1 indicates that the compound is more toxic to the pathogenic bacteria than to human cells.

To determine whether squalamine has a bactericidal action, we also performed bactericidal assays. Bacteria were first incubated for 18 hours with the drug at 0, 1, 2 and 4 times the MIC concentration and then 100 µL were plated on agar plates following serial dilutions from 10^{-1} to 10^{-7} (Fig. 2A SI). The bactericidal effect was estimated by comparing the number of colonies forming units (CFU~~, *i.e.* viable cells~~) to the initial inoculum (5 X 10^6 CFU/mL). Bactericidal activity was defined as a reduction of at least 3 $\log_{10}$ (≥ 99,9%) of the total CFU/mL in the original inoculum. For all tested squalamine concentrations, a decrease of viable cells (CFU) was observed and no cells were detected at dilutions 10^{-4}, 10^{-3} and 10^{-2} for squalamine at MIC, 2 MIC and 4 MIC, respectively (Fig. 2B SI). The absence of growth on culture media without drug after the drug exposure in liquid for 18h document on the bactericidal effect of squalamine on *S. epidermidis*. We observe a decrease of the bacterial

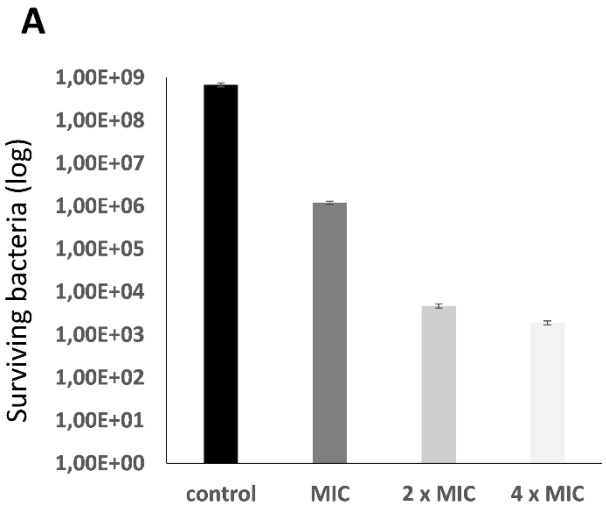

B

Squalamine

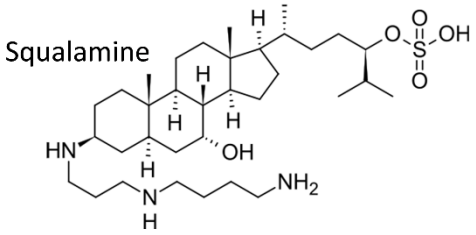

Spermidine

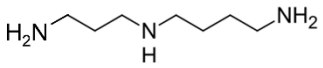

	Squalamine	Spermidine
MIC	2 µg/mL	>2560 µg/mL

load close to 3 $\log_{10}$ which clearly indicates a bactericidal activity (Fig. 2A). On the opposite, there was no MIC or bactericidal effect on *S. epidermidis* for the spermidine at the maximal tested concentration of 2560 µg/mL (MIC >2560 µg/ mL, Fig. 1B).

Figure 1. Bactericidal assay for the squalamine and chemical structures of the molecules used in this study. (A) Panel showing the progressive loss of viability (%) of squalamine–treated *S. epidermidis* at MIC, 2 x MIC and 4 x MIC (grey bars), respectively. The untreated growth control (black bar) exhibited the expected uninhibited growth. (B) Chemical structure of squalamine and spermidine together with the values of MIC determined for the two molecules.

Squalamine affects *S. epidermidis* peptidoglycan structure and compromise its permeability.

The action of squalamine on Gram-negative bacteria has been well-described as binding to the LPS and further disrupting the membrane of the cells due to a detergent-like effect and micellization [15]. Very recently, Boes *et al.* have also discovered another function where squalamine would inhibit the activity of enzymes involved in the peptidoglycan synthesis of *Escherichia coli* [16]. On the other hand, very few studies relate the squalamine mechanisms of action on Gram-positive bacteria. By using a combination of ATP release measurements, TEM and fluorescence assays, Alhanout *et al.* in 2010 have reported a strong depolarization of the membrane of *Staphylococcus aureus* and *Streptococcus pneumoniae* [13]. However, to our knowledge, no further mechanisms have been described on Gram-positive bacteria.

To better understand the effect of squalamine on *S. epidermidis* at the bacterial suspension scale, permeability assay has been performed using N-phenyl-1-naphthylamine (NPN), a dye which becomes fluorescent in hydrophobic environments such as membranes (Fig. 2). As seen in Fig. 2B, the fluorescence level before treatment was low, meaning that the dye had no access to the membrane because of peptidoglycan (PG) low permeability. After culturing the bacteria with a sub-lethal concentration of squalamine, the fluorescence intensity of NPN became significantly increased documenting that the drug permeabilised *S. epidermidis* cell wall most likely by de-structuring the peptidoglycan (Fig. 2B, C).

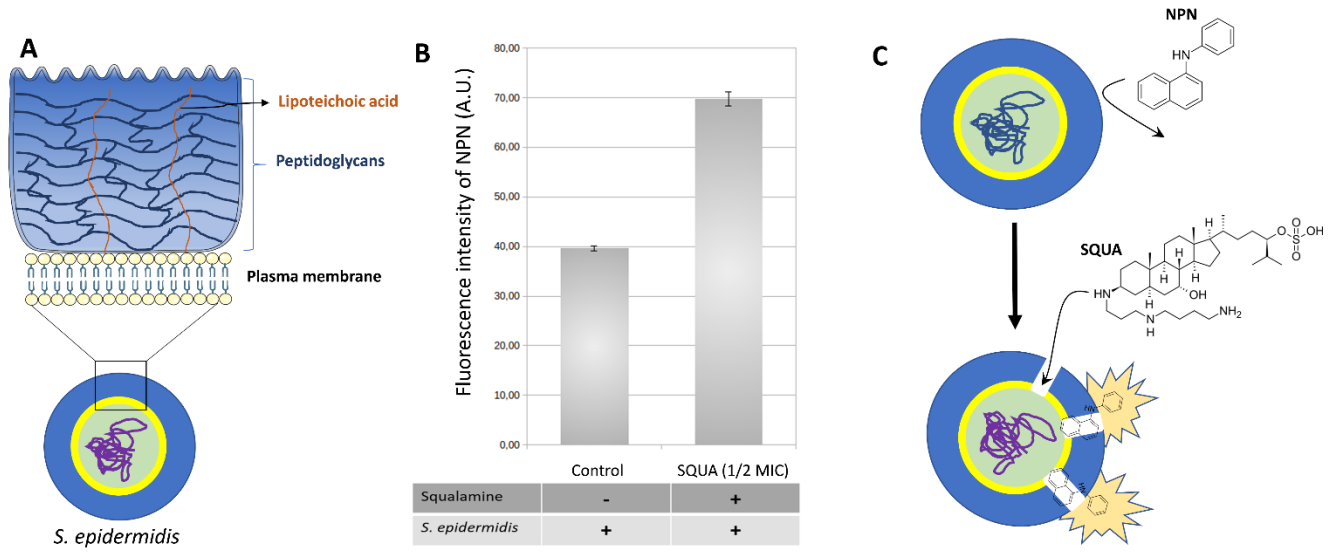

Figure 2. Methodology used to determine interactions of Squalamine (SQUA) with *S. epidermidis* membranes using N-phenyl-1-naphthylamine (NPN) permeability assay. The fluorescent NPN dye can be used to monitor the integrity of the bacterial membrane. (A) Schematic representation of the essential elements of the structure of the Gram-positive cocci *S. epidermidis*, with inner plasma membrane (yellow), peptidoglycan layer (blue) with lipoteichoic acid (orange) and peptidoglycans (dark blue), intracellular content (green) and nucleic acids (purple). (B) Graph showing fluorescence measurement before and after addition of Squalamine in *S. epidermidis* culture. *S. epidermidis* was exposed to SQUA at 0.5 MIC (1 µM), and the permeability of the bacterial membrane was monitored by measuring the fluorescence of NPN. Fluorescence values were compared to untreated bacteria, in a media control. Panel I of the graph shows the fluorescence level of control bacteria without damaged membrane (Control). Panel II indicates possible partial permeabilization of bacterial membrane by SQUA, resulting in an increase of fluorescence readings after addition of NPN. (C) Illustration of a model of how SQUA could affect the permeability of the membrane in *S. epidermidis*. The fluorescent dye NPN before (top) and after (bottom) treatment of *S. epidermidis* with SQUA. NPN becomes fluorescent when in hydrophobic environment such as membranes, after an induced damage. A sub-lethal concentration of SQUA makes the membrane of *S. epidermidis* more permeable. NPN is excluded from untreated bacteria but penetrates into *S. epidermidis* with a compromised cell wall where it binds, resulting in increased fluorescence.

We then used AFM to get a closer look to the squalamine effect on the bacterial cell wall at the cellular scale. AFM images of *S. epidermidis* before and after treatment with squalamine at twice the MIC for 12 h are depicted on Fig. 3. Without drug treatment, individual cells images obtained in buffer appeared round and homogeneous (Fig. 3A). Images acquired at

higher magnification and roughness analysis indicate that the bacterial surface is smooth (rms roughness = 1.2 ± 0.5 nm).

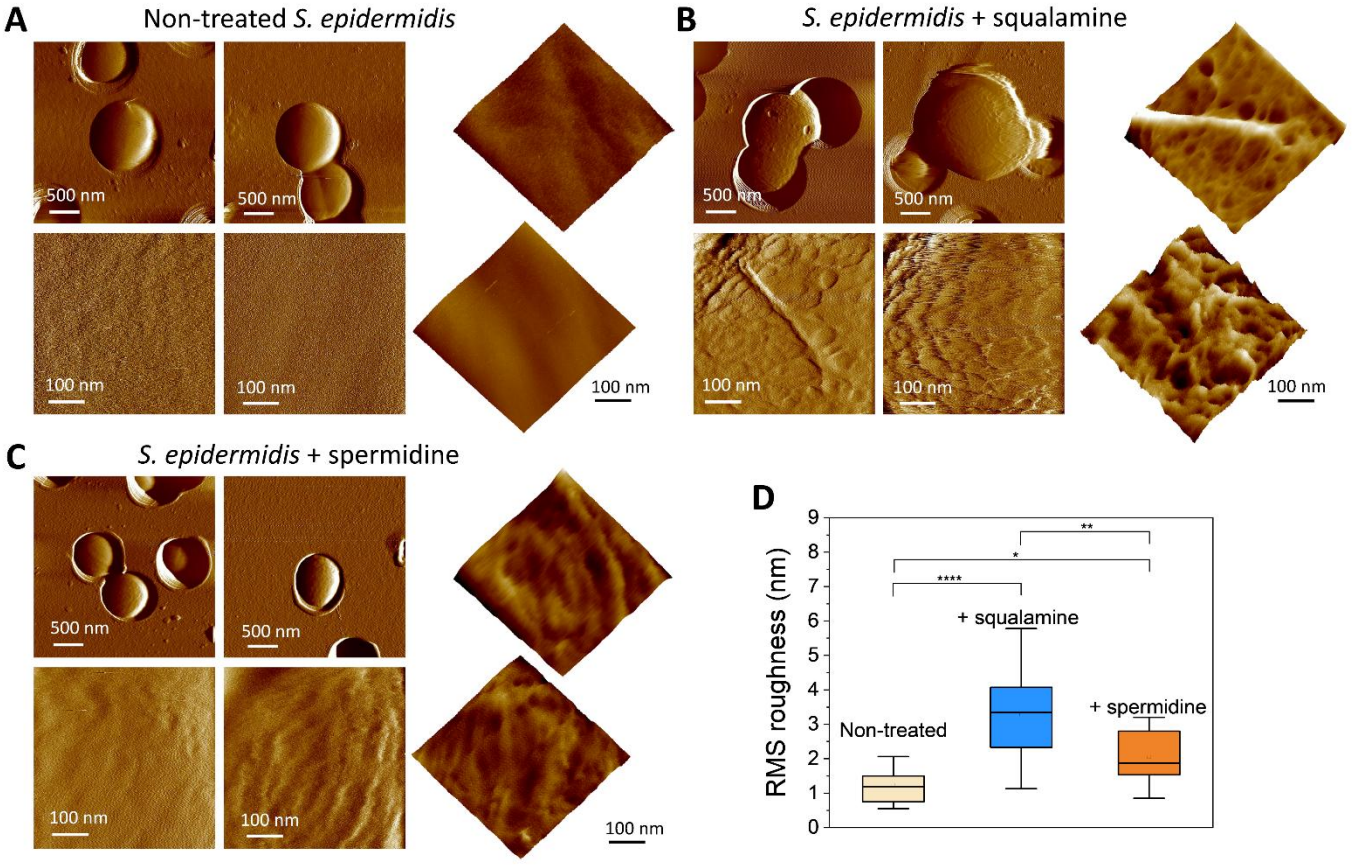

At 2x MIC of squalamine, some bacteria presented abnormal bigger size as compared to the non-treated cells (1445 ± 219 nm for squalamine-treated cells *vs* 929 ± 70 nm for non-treated cells) and all cells displayed some bumps and holes at their surface (Fig. 3B), increasing the average roughness to 3.3 ± 1.3 nm.

Figure 3. AFM images of native, squalamine- and spermidine-treated *S. epidermidis* cells. (A-D) Low (top) and high (bottom) magnification deflection images in 2D (left) and 3D (right) of *S. epidermidis* acquired in buffer solution for non-treated cells (A), and cells cultured overnight with 4 µM of squalamine (B) and 4 µM of spermidine (C). (D) Classical whisker representation of the root mean square (RMS) roughness extracted from AFM images, for which the bottom and the top of the box are the 25th and the 75th percentiles. The black band in the box corresponds to the median. Data in panel D stem from measurements conducted at least on 11 different bacteria (probed cell surface area 500 × 500 nm^2). Statistical analysis using Welch's Anova test (*: $p < 0.05$, **: $p < 0.01$, ***: $p < 0.001$, ****: $p < 0.0001$), resulting in p values of <0.0001 for native *vs* squalamine-

treated cells, 0.0118 for native *vs* spermidine-treated cells, and 0.0045 for squalamine- *vs* spermidine-treated cells.

Closer inspection of the morphology of the treated bacteria revealed a tight disorder mesh composed of pores, recalling that of peptidoglycan mature *S. aureus* cells [17], even more visible in the 3D representation of the images (Fig. 3B). We thus hypothesis that squalamine might i) have a direct impact by abrading the cell wall biomolecules, bringing out the PG structure and/or ii) act intracellularly by modifying PG synthesis pathway – as it has been reported for Gram-negative bacteria.[16] However, this hypothesis was not chemically confirmed.

Performing the same AFM image analysis on *S. epidermidis* treated with an equivalent concentration in spermidine (conc= 4 µM; Fig. 3C) showed that spermidine has only little influence on the bacteria shape and surface roughness (rms = 2.1 ± 0.7 nm), confirming that the integrity of the squalamine molecule needs to be conserved for its antimicrobial effect.

Squalamine binds to *S. epidermidis* surface *via* its spermidine segment.

We then used single-molecule force spectroscopy (SMFS) to decipher squalamine adhesion mechanisms and address the following question: by which segment of the molecule is squalamine binding to the bacterial surface?

For that, AFM tips were first decorated with squalamine using a covalent linking chemistry. Fig. 4A display adhesion maps obtained on 4 different bacteria using 4 independent tips, together with the adhesion and rupture length histograms obtained from the 4096-individual force-distance curves pooled from the 4 experiments. The majority of the force-distance curves (95 %) showed adhesion signatures, with adhesion force ranging from 50 to 300 pN and rupturing around 300 nm. Interestingly, two types of force profiles could be

observed, as depicted on representative curves on Fig. 4A: low adhesion force profile with single or very few irregular peaks at small adhesion force and short rupture length (69 % of the total force curves), whereas 26 % of the force-distance curves display very distinct sawtooth patterns. ~~A detailed analysis of the origin of these peculiar profiles is described in the next paragraph.~~

Interestingly, almost the same results were obtained when decorating the AFM tips with only the spermidine segment, resulting in a total of 98 % adhesive force-distance curves with 70 % of single/small adhesion and 28 % of sawtooth pattern curves (Fig. 4B).

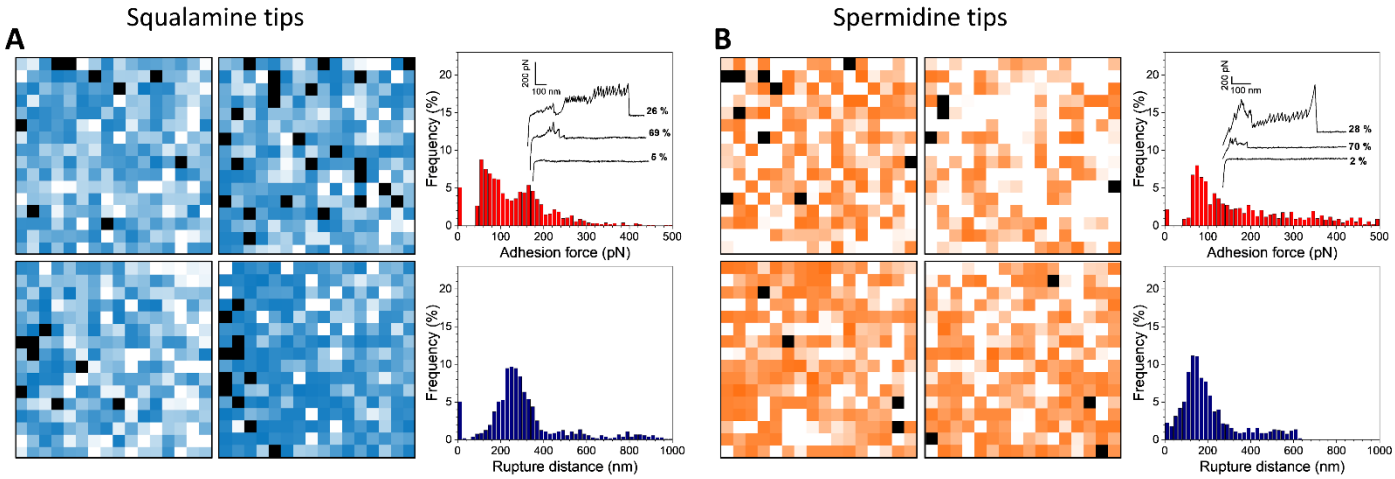

Figure 4. Squalamine adheres to *S. epidermidis* surface *via* the spermidine motif. (A; B) Adhesion force maps (250 × 250 nm^2, black and colored pixels correspond to adhesion forces smaller and larger than 50 pN, respectively. Brighter colors mean larger adhesion; color scale: 250 pN) recorded in buffer between the surface of *S. epidermidis* cells and AFM tips functionalized with squalamine (A) and spermidine (B). The 4 maps correspond to 4 different AFM tips adhering on 4 bacteria from independent cultures. The histograms correspond to the frequency of adhesion force (top) and rupture distances (bottom) constructed from 1024 force-distance curves pooled from data from the 4 depicted maps, together with representative force-distance curves and their frequency of appearance.

At the opposite, using bare tips (Fig. 5A) or hydrophobic tips (Fig. 5B) result in a very poor adhesion frequency where multipeak signatures were never observed. Altogether, our SMFS results indicate that squalamine adheres strongly and homogeneously at the surface of *S. epidermidis via* the spermidine motif, most likely *via* electrostatic interaction between the

positively-charged amine group of spermidine and the negatively-charged bacterial surface, and that the function of the hydrophobic sterol-group is not related to surface attachment.

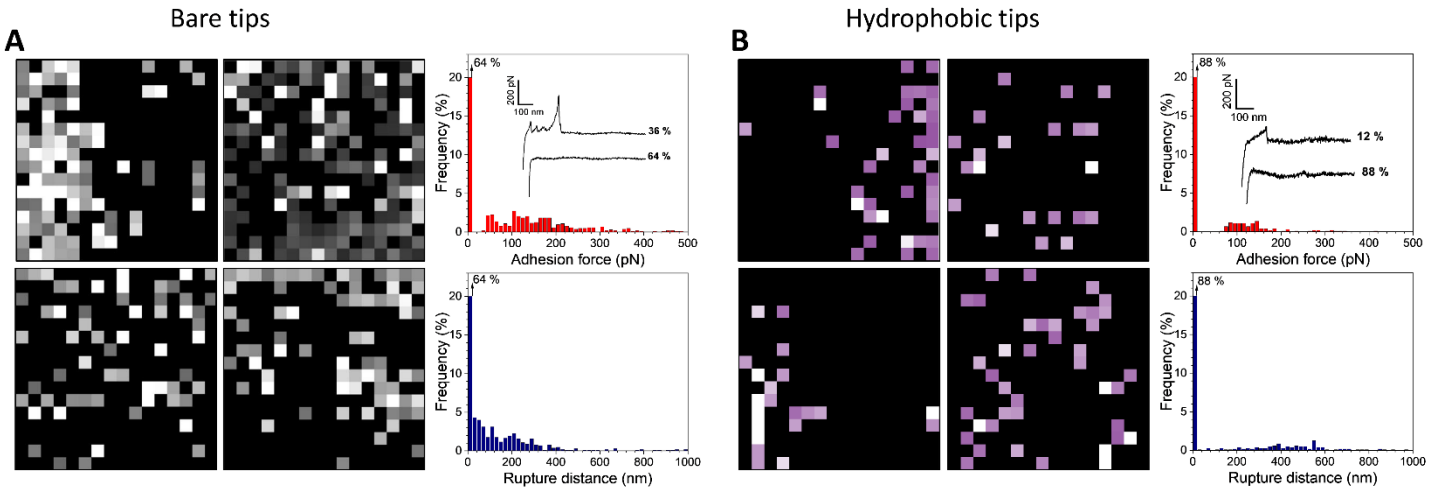

Figure 5. The hydrophobic part of squalamine do not play a role in the initial adhesion to the biosurface. (A; B) Adhesion force maps (250 × 250 nm^2, black and colored pixels correspond to adhesion forces smaller and larger than 50 pN, respectively. Brighter colors mean larger adhesion; color scale: 250 pN) recorded in buffer between the surface of *S. epidermidis* cells and AFM bare tips as received from the supplier (A) and AFM tips decorated with hydrophobic-thiols (B). The 4 maps correspond to 4 different AFM tips adhering on 4 bacteria from independent cultures. The histograms correspond to the frequency of adhesion force (top) and rupture distances (bottom) constructed from 1024 force-distance curves pooled from data from the 4 depicted maps, together with representative force-distance curves and their frequency of appearance.

The *S. epidermidis* adhesin Aap is involved in the adhesion of squalamine to the bacteria.

As mentioned above, about one quarter of the force-distance curves recorded between squalamine- or sperdimine-decorated tips and the surface of *S. epidermidis* display very regular sawtooth patterns (Fig. 4, Fig 6A). These patterns are reminiscent of that described when stretching the adhesin SasG at the surface of *Staphylococcus aureus* [18] and Aap at the surface of *S. epidermidis* [19], *i.e.* being composed of a series of low force peaks (178 ± 6 pN) followed by series of high force peaks (248 ± 15 pN) (Fig. 6B). Fitting the peaks with the worm-like-chain (WLC) model allows to extract the length of the extended molecule,[20] so-called the contour length L_c. Statistical analysis of the increase of contour length ΔL_c revealed

an increment of 20 ± 1 nm for the low-force peaks and of 29 ± 1 nm for the high-force peaks (Fig. 6C), in full agreement with the number of aa constituting the E and G5 domains of the Aap

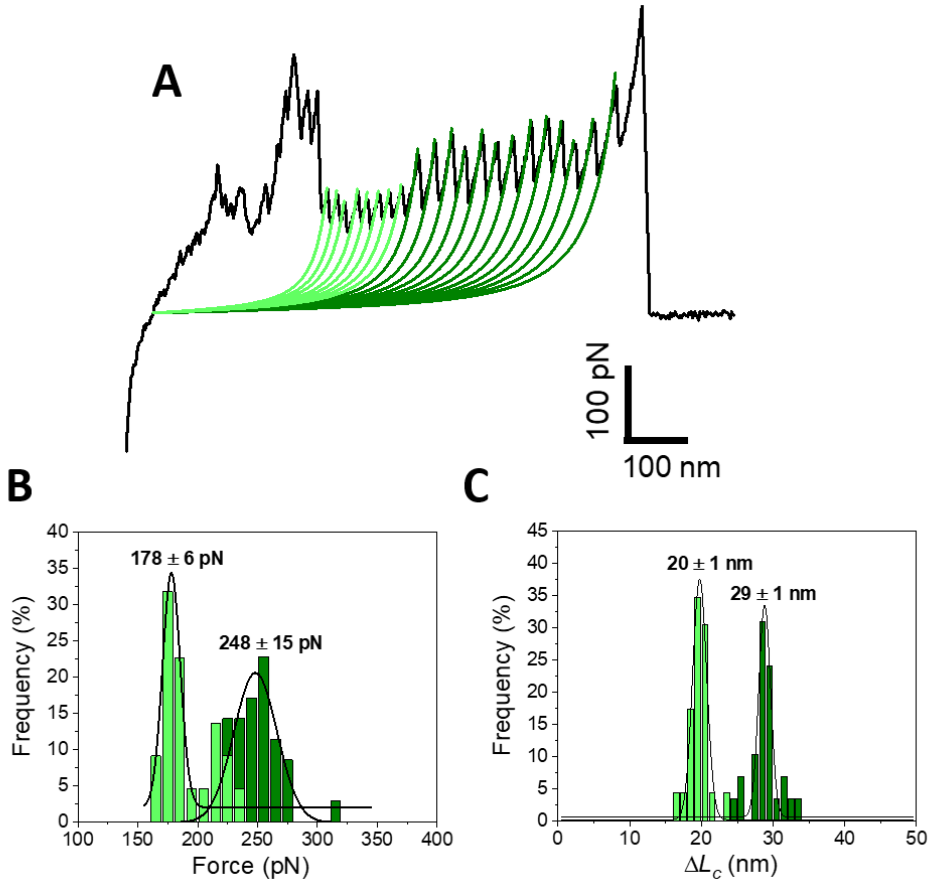

protein, *i.e.* 48 aa and 72 aa respectively, assuming that each aa contributes 0.4 nm (48 x 0.4 = 19.2 nm and 72 x 0.4 = 28.8 nm).

Figure 6. Squalamine binding to *S. epidermidis* leads to the unfolding of Aap proteins. (A) Representative force-distance curve displaying sawtooth patterns (black), where each peak can be fitted by the Worm-like chain (WLC) model (green curves). (B, C) Unfolding force (B) and increase of contour length ΔL_c (C) of the peaks for the sawtooth-pattern curves display bimodal distribution, corresponding to the E domains (light green) and G5 domains (dark green) of the Aap protein at the surface of *S. epidermidis.*

Conclusions

Squalamine is among a new class of antibiotics of animal origin which has been reported as being efficient against multi-resistant bacteria. Although this natural product offers exciting perspectives, its mechanisms of action are not fully elucidated yet. Here, we used biological assays combined to the AFM multifunctional platform to better understand how squalamine binds to and affects the cell wall of the nosocomial pathogenic *S. epidermidis*. We revealed that the accumulation-associated protein (Aap) at the surface of *S. epidermidis* is involved in the initial binding of squalamine to the bacterial cell wall, *via* the spermidine motif of the drug.

This study contributes to elucidate how squalamine acts on individual bacteria, which is a necessary step to go deeper in the understanding of the remarkable efficiency and multi-facetted properties of squalamine as antimicrobial agent.

ACKNOWLEDGMENTS

We thank the Groupement de Recherche GDR Imabio from CNRS for supporting the internship of E. Salles. The authors would like to acknowledge also the financial support by Institut Jean Barriol. We thank the Spectroscopy and Microscopy of interfaces Service Facility (SMI) of LCPME (Université de Lorraine-CNRS–(www.lcpme.cnrs-nancy.fr); LCPME, UMR7564, 405 rue de Vandoeuvre 54600, France). This work was partly carried out in the Pôle de compétences Physico-Chimie de l'Environnement, LIEC laboratory UMR 7360 CNRS – Université de Lorraine.

Author contributions: SEKC, MV and AB designed the research and wrote the manuscript; SEKC, MV, CR, ES, AR, J-M B and AB contributed to the acquisition, analysis, and interpretation of the data. SEKC, MV, CR, ES, AR, J-M B and AB revised the paper and all authors approved the final version.

Conflicts of Interest: The authors declare no conflict of interest.

References

1. Otto, M. *Staphylococcus epidermidis*-the 'accidental' pathogen. *Nat Rev Microbiol* **2009**, *7,* 555-567.
2. Otto, M. Staphylococcal infections: mechanisms of biofilm maturation and detachment as critical determinants of pathogenicity. *Annu Rev Med* **2013**, *64,* 175-188.
3. Foster, T.J. Surface Proteins of *Staphylococcus epidermidis. Front Microbiol* **2020**, *11,* 1829.
4. Los, R.; Sawicki, R.; Juda, M.; Stankevic, M.; Rybojad, P.; Sawicki, M.; Malm, A.; Ginalska, G. A comparative analysis of phenotypic and genotypic methods for the determination of the biofilm-forming abilities of *Staphylococcus epidermidis. FEMS Microbiol Lett* **2010**, *310,* 97-103.
5. Mack, D.; Becker, P.; Chatterjee, I.; Dobinsky, S.; Knobloch, J.K.; Peters, G.; Rohde, H.; Herrmann, M. Mechanisms of biofilm formation in *Staphylococcus epidermidis* and Staphylococcus aureus: functional molecules, regulatory circuits, and adaptive responses. *Int J Med Microbiol* **2004**, *294,* 203-212.
6. Rohde, H.; Burdelski, C.; Bartscht, K.; Hussain, M.; Buck, F.; Horstkotte, M.A.; Knobloch, J.K.; Heilmann, C.; Herrmann, M.; Mack, D. Induction of *Staphylococcus epidermidis* biofilm

formation via proteolytic processing of the accumulation-associated protein by staphylococcal and host proteases. *Mol Microbiol* **2005**, *55,* 1883-1895.
7. Conrady, D.G.; Brescia, C.C.; Horii, K.; Weiss, A.A.; Hassett, D.J.; Herr, A.B. A zinc-dependent adhesion module is responsible for intercellular adhesion in staphylococcal biofilms. *Proc Natl Acad Sci U S A* **2008**, *105,* 19456-19461.
8. Lee, J.Y.H.; Monk, I.R.; Goncalves da Silva, A.; Seemann, T.; Chua, K.Y.L.; Kearns, A.; Hill, R.; Woodford, N.; Bartels, M.D.; Strommenger, B.; Laurent, F.; Dodemont, M.; Deplano, A.; Patel, R.; Larsen, A.R.; Korman, T.M.; Stinear, T.P.; Howden, B.P. Global spread of three multidrug-resistant lineages of *Staphylococcus epidermidis. Nat Microbiol* **2018**, *3,* 1175-1185.
9. Alhanout, K.; Rolain, J.M.; Brunel, J.M. Squalamine as an example of a new potent antimicrobial agents class: a critical review. *Curr Med Chem* **2010**, *17,* 3909-3917.
10. Kazakova, O.; Giniyatullina, G.; Babkov, D.; Wimmer, Z. From Marine Metabolites to the Drugs of the Future: Squalamine, Trodusquemine, Their Steroid and Triterpene Analogues. *Int J Mol Sci* **2022**, *23*.
11. Mammari, N.; Salles, E.; Beaussart, A.; El-Kirat-Chatel, S.; Varbanov, M. Squalamine and Its Aminosterol Derivatives: Overview of Biological Effects and Mechanisms of Action of Compounds with Multiple Therapeutic Applications. *Microorganisms* **2022**, *10*.
12. Salmi, C.; Loncle, C.; Vidal, N.; Letourneux, Y.; Fantini, J.; Maresca, M.; Taieb, N.; Pages, J.M.; Brunel, J.M. Squalamine: an appropriate strategy against the emergence of multidrug resistant gram-negative bacteria? *PLoS One* **2008**, *3,* e2765.
13. Alhanout, K.; Malesinki, S.; Vidal, N.; Peyrot, V.; Rolain, J.M.; Brunel, J.M. New insights into the antibacterial mechanism of action of squalamine. *J Antimicrob Chemother* **2010**, *65,* 1688-1693.
14. Mosmann, T. Rapid colorimetric assay for cellular growth and survival: application to proliferation and cytotoxicity assays. *J Immunol Methods* **1983**, *65,* 55-63.
15. Di Pasquale, E.; Salmi-Smail, C.; Brunel, J.M.; Sanchez, P.; Fantini, J.; Maresca, M. Biophysical studies of the interaction of squalamine and other cationic amphiphilic molecules with bacterial and eukaryotic membranes: importance of the distribution coefficient in membrane selectivity. *Chem Phys Lipids* **2010**, *163,* 131-140.
16. Boes, A.; Brunel, J.M.; Derouaux, A.; Kerff, F.; Bouhss, A.; Touze, T.; Breukink, E.; Terrak, M. Squalamine and Aminosterol Mimics Inhibit the Peptidoglycan Glycosyltransferase Activity of PBP1b. *Antibiotics (Basel)* **2020**, *9*.
17. Pasquina-Lemonche, L.; Burns, J.; Turner, R.D.; Kumar, S.; Tank, R.; Mullin, N.; Wilson, J.S.; Chakrabarti, B.; Bullough, P.A.; Foster, S.J.; Hobbs, J.K. The architecture of the Gram-positive bacterial cell wall. *Nature* **2020**, *582,* 294-297.
18. Formosa-Dague, C.; Speziale, P.; Foster, T.J.; Geoghegan, J.A.; Dufrene, Y.F. Zinc-dependent mechanical properties of *Staphylococcus aureus* biofilm-forming surface protein SasG. *Proc Natl Acad Sci U S A* **2016**, *113,* 410-415.
19. Chantraine, C.; Mathelie-Guinlet, M.; Pietrocola, G.; Speziale, P.; Dufrene, Y.F. AFM Identifies a Protein Complex Involved in Pathogen Adhesion Which Ruptures at Three Nanonewtons. *Nano Lett* **2021**, *21,* 7595-7601.
20. Rief, M.; Gautel, M.; Oesterhelt, F.; Fernandez, J.M.; Gaub, H.E. Reversible unfolding of individual titin immunoglobulin domains by AFM. *Science* **1997**, *276,* 1109-1112.
21. Schaeffer, C.R.; Woods, K.M.; Longo, G.M.; Kiedrowski, M.R.; Paharik, A.E.; Buttner, H.; Christner, M.; Boissy, R.J.; Horswill, A.R.; Rohde, H.; Fey, P.D. Accumulation-associated protein enhances *Staphylococcus epidermidis* biofilm formation under dynamic conditions and is required for infection in a rat catheter model. *Infect Immun* **2015**, *83,* 214-226.
22. Yarawsky, A.E.; Herr, A.B. The staphylococcal biofilm protein Aap forms a tetrameric species as a necessary intermediate before amyloidogenesis. *J Biol Chem* **2020**, *295,* 12840-12850.
23. Yarawsky, A.E.; Johns, S.L.; Schuck, P.; Herr, A.B. The biofilm adhesion protein Aap from *Staphylococcus epidermidis* forms zinc-dependent amyloid fibers. *J Biol Chem* **2020**, *295,* 4411-4427.

24. Limbocker, R.; Staats, R.; Chia, S.; Ruggeri, F.S.; Mannini, B.; Xu, C.K.; Perni, M.; Cascella, R.; Bigi, A.; Sasser, L.R.; Block, N.R.; Wright, A.K.; Kreiser, R.P.; Custy, E.T.; Meisl, G.; Errico, S.; Habchi, J.; Flagmeier, P.; Kartanas, T.; Hollows, J.E.; Nguyen, L.T.; LeForte, K.; Barbut, D.; Kumita, J.R.; Cecchi, C.; Zasloff, M.; Knowles, T.P.J.; Dobson, C.M.; Chiti, F.; Vendruscolo, M. Squalamine and Its Derivatives Modulate the Aggregation of Amyloid-beta and alpha-Synuclein and Suppress the Toxicity of Their Oligomers. *Front Neurosci* **2021**, *15,* 680026.